

Article

Carbonic Anhydrase Inhibition with Sulfonamides Incorporating Pyrazole- and Pyridazincarboxamide Moieties Provides Examples of Isoform-Selective Inhibitors

Andrea Angeli ^{1,2} , Victor Kartsev ³, Anthi Petrou ⁴ , Mariana Pinteala ² , Volodymyr Brovarets ⁵, Roman Vydzhak ⁵ , Svitlana Panchishin ⁵ , Athina Geronikaki ^{4,*}  and Claudiu T. Supuran ^{1,*} 

¹ NeuroFarba Department, Sezione di Scienze Farmaceutiche, Università degli Studi di Firenze, Via Ugo Schiff 6, 50019 Sesto Fiorentino, Italy; andrea.angeli@unifi.it

² Centre of Advanced Research in Bionanoconjugates and Biopolymers, Petru Poni Institute of Macromolecular Chemistry, Aleea Grigore Ghica-Voda, no. 41A, 700487 Iasi, Romania; pinteala@icmpp.ro

³ InterBioScreen, Chernogolovka, 142432 Moscow Region, Russia; vkartsev@ibscreen.chg.ru

⁴ Department of Pharmacy, School of Health, Aristotle University of Thessaloniki, 54124 Thessaloniki, Greece; anthi.petrou.thessaloniki1@gmail.com

⁵ Department of Chemistry of Bioactive Nitrogen-Containing Heterocyclic Bases, V.P. Kukhar Institute of Bioorganic Chemistry and Petrochemistry, NAS of Ukraine 1, Murmanska St, 02094 Kyiv, Ukraine; brovarets@bpci.kiev.ua (V.B.); rmvydzhak@gmail.com (R.V.); svpanch@ukr.net (S.P.)

* Correspondence: geronik@pharm.auth.gr (A.G.); claudiu.supuran@unifi.it (C.T.S.)



Citation: Angeli, A.; Kartsev, V.; Petrou, A.; Pinteala, M.; Brovarets, V.; Vydzhak, R.; Panchishin, S.; Geronikaki, A.; Supuran, C.T. Carbonic Anhydrase Inhibition with Sulfonamides Incorporating Pyrazole- and Pyridazincarboxamide Moieties Provides Examples of Isoform-Selective Inhibitors. *Molecules* **2021**, *26*, 7023. <https://doi.org/10.3390/molecules26227023>

Academic Editor:
Diego Muñoz-Torrero

Received: 28 October 2021
Accepted: 18 November 2021
Published: 20 November 2021

Publisher's Note: MDPI stays neutral with regard to jurisdictional claims in published maps and institutional affiliations.



Copyright: © 2021 by the authors. Licensee MDPI, Basel, Switzerland. This article is an open access article distributed under the terms and conditions of the Creative Commons Attribution (CC BY) license (<https://creativecommons.org/licenses/by/4.0/>).

Abstract: A series of benzenesulfonamides incorporating pyrazole- and pyridazincarboxamides decorated with several bulky moieties has been obtained by original procedures. The new derivatives were investigated for the inhibition of four physiologically crucial human carbonic anhydrase (hCA, EC 4.2.2.1.1) isoforms, hCA I and II (cytosolic enzymes) as well as hCA IX and XII (transmembrane, tumor-associated isoforms). Examples of isoform-selective inhibitors were obtained for all four enzymes investigated here, and a computational approach was employed for explaining the observed selectivity, which may be useful in drug design approaches for obtaining inhibitors with pharmacological applications useful as antiglaucoma, diuretic, antitumor or anti-cerebral ischemia drugs.

Keywords: carbonic anhydrase; inhibitors; metalloenzymes; pyrazole derivatives

1. Introduction

The proper function of physiological processes in the human body depends on the preservation of an adequate acid–base balance. Indeed, the normal intracellular pH range is between 7.35 and 7.45, but when the pH deviates from this range, pathological conditions are commonly observed [1]. CO₂ is generated and used in many metabolic reactions, and one of the most important buffer systems used by cells is the homeostatic HCO₃[−]/CO₂ mechanism. Because of the slow reaction between CO₂ and H₂O, enzymes are fundamental to speed up the process; for example, carbonic anhydrases (CAs, EC 4.2.1.1) are efficient catalysts for the reversible reaction between CO₂ and HCO₃[−] [2]. To date this class of enzymes has been divided into eight distinct and genetically unrelated families [3–6]. In humans, there are 15 isoforms, and their overexpression is often related to different diseases. Indeed, the abnormal expression of CA I, IV, IX, and XII isoforms in serum and synovium specimens are related to rheumatoid arthritis, and their overexpression also has been demonstrated to negatively affect cellular immunity processes and to enhance associated symptoms [7–9]. In addition, the overexpression of hCA IX and XII was observed in several cancer diseases, as well as in patients suffering from cerebral ischemia [3,10–12].

In this context, the pyrazole scaffold is a versatile molecule that has attracted attention due to its wide range of diverse pharmacological activities, which make it a versatile lead

molecule in several drug molecules such as celecoxib, ramifenazone, lonazolac, and rimonabant, drugs approved as COX-2 inhibitors [13–16], crizotinib [17] and paropanib [17] as anticancer drugs, sildenafil [17] (Viagra) PDE5 inhibitor, zometapine [18] as antidepressant, ocinaplon [19] as anxiolytic (Figure 1), and many others. Additionally, in recent years, their derivatives have been reported to possess antimicrobial activity [20–22] as well as antiviral [23,24], antidiabetic [25,26], anti-Alzheimer [27,28], antitubercular [29,30], and antileishmanial properties [31].

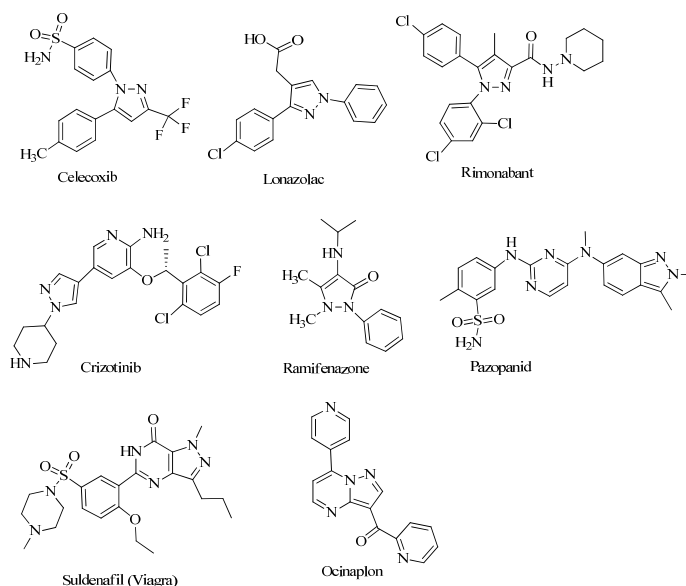


Figure 1. Structure of drugs bearing the pyrazole moiety.

Our aim was to further support our previous studies on hCAs as valid and robust pharmacological targets for the treatment of different pathological conditions that are characterized by the overexpression of different human CA isoforms such as CA IX and XII over the ubiquitous hCA I and hCA II in order to decrease the side effects due to their inhibition, such as with the clinically approved drug acetazolamide (AAZ) depicted in Figure 2.

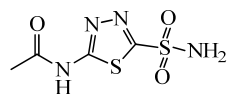
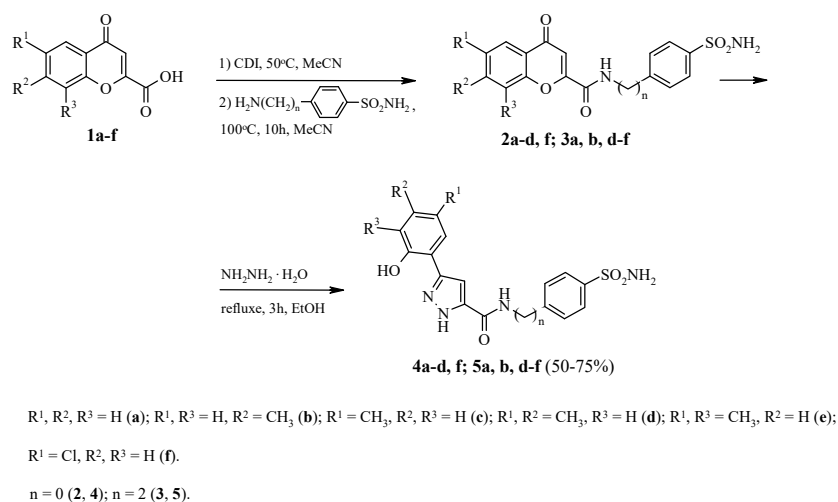


Figure 2. Structure of acetazolamide (AAZ).

2. Results

2.1. Chemistry

The synthesis of target compounds **4** and **5** is presented in Scheme 1. Starting 4-oxo-4H-chromene-2-carboxylic acids **1** [32,33] were initially converted into substituted amides **2** and **3**, which without further purification were used for the preparation of pyrazole derivatives **4a–d,f** and **5a,b,d–f**. Some examples of such transformations of 4-oxo-4H-chromene-2-carboxamides to substituted pyrazoles were also described earlier [34].



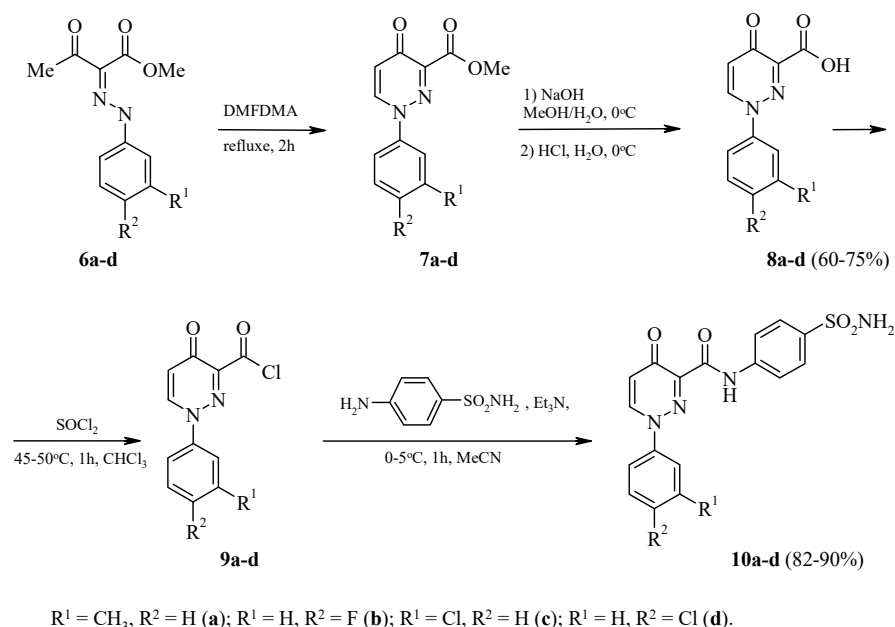
Scheme 1. Synthesis of 3-(2-hydroxyaryl)-1H-pyrazole derivatives.

The structure and composition of compounds **4a–d,f** and **5a,b,d–f** were confirmed by 1H , ^{13}C NMR spectroscopy and elemental analysis (see Supplementary Materials). The signals of all observed in the 1H NMR spectra protons appear in usual spectral regions that unambiguously correspond to the structure of the synthesized substances. For compound **5a** 1H NMR, spectra were recorded in solutions of DMSO- d_6 , CF_3COOD and DMSO- d_6 + 5% (mass) CF_3SO_3H . It should be noted that, obviously, compound **5a** predominantly exists as two tautomeric forms in the solution of DMSO- d_6 . In this case, a double set of signals of the OH group (13.78 s, 0.35H and 13.17 s, 0.65H), NH pyrazole fragment (10.39 s, 0.35H and 10.20 s, 0.65H) and NH carboxamide group (8.69 s, 0.35H and 8.13 s, 0.65H) was observed, while the signals of aromatic protons of hydroxyaryl substituents, 4-H pyrazole moiety and aliphatic groups appeared as broad multiplets and the signals of the arylsulfamide moiety were clearly separated and resolved at 7.28 (s, 2H, NH_2).

In the 1H NMR spectra of compound **5a**, measured in CF_3COOD , OH and NH proton signals were not detected; at the same time, the aromatic and aliphatic signals were more clearly separated and resolved, although some of their broadening was also observed. In the spectrum of compound **5a** measured in DMSO- d_6 + 5% (mass) CF_3SO_3H , signals of protons of NH-pyrazole, hydroxy and aminosulfonyl groups were not detected, whereas the signals of aromatic and aliphatic protons were more clearly resolved and separated. Signals of aromatic protons of the arylsulfamide fragment were at 7.73 (d, $J = 8.0$ Hz, 2H, Ar) and 7.41 (d, $J = 8.0$ Hz, 2H, Ar). The signal of 4-pyrazole was superimposed with the signal of the orthohydroxyphenyl substituent at 7.24–7.11 ppm. At the same time, the NH signal of the carboxamide group of **5a** (8.45 s, 1H, NH) was clearly observable. In the NMR 1H spectra of compounds **4a–d,f** and **5b,d–f** recorded in DMSO- d_6 and DMSO- d_6 + 5% (mass) CF_3SO_3H , there was a set of signals similar to the corresponding set of signals in the NMR 1H spectra of compound **5a** measured in the same solvents. Measurement of the ^{13}C NMR spectra of compound **5a** in DMSO- d_6 or CF_3COOD gave low-resolved or undefined peaks, while in spectra recorded in the solution of DMSO- d_6 + 5% (mass) CF_3SO_3H , all the signals of carbon atoms (the number of corresponding to the number of carbon atoms in their structure) appeared as well-defined and highly resolved peaks.

Probably, the addition of a small amount of trifluoromethanesulfonic acid (as one of the strongest acids) is sufficient for the protonation of the pyrazole ring, which leads to an increase in the proton exchange rate, resulted in obtaining the more highly resolved and clearly defined spectra. Additionally, in the ^{13}C NMR spectra, a quartet of trifluoromethyl group (clearly separated from the signals of the carbon atoms of compounds **4a–d, f** and **5a, b, d–f**) appeared. Molecular ion peaks $[M+H]^+$ and $[M-H]^-$ are usually detected in LC/MS spectra of the compounds **4, 5**.

N-[4-(aminosulfonyl) phenyl]-1-aryl-4-oxo-1,4-dihydropyridazine-3-carboxamides **10** were synthesized according to the pathway shown in Scheme 2. Methyl 4-oxo-1-aryl-1,4-dihydropyridazine-3-carboxylates **7** were obtained by refluxing the corresponding methyl 3-oxo-2-(arylhrazono)butanoates **6** in DMFDMA [35–37], and their further hydrolysis led to 4-oxo-1-aryl-1,4-dihydropyridazine-3-carboxylic acids **8** [36,37]; then, **8** were converted into appropriate acid chlorides **9**; finally, treatment with aromatic amines yielded **10a–d**.

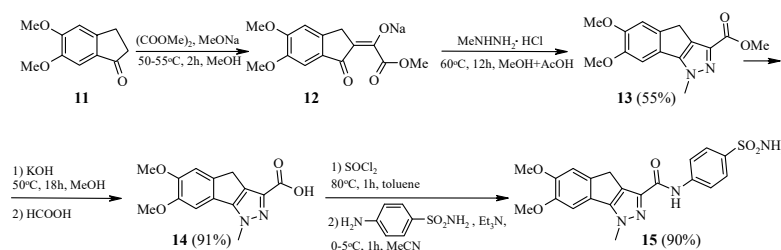


Scheme 2. Synthesis of 1-aryl-4-oxo-1,4-dihydropyridazine derivatives.

The structure and composition of compounds **8a–d** and **10a–d** were confirmed by ^1H , ^{13}C NMR spectroscopy and elemental analysis. The signals of the 1-aryl-4-oxo-1,4-dihydropyridazine moiety of compounds **8** and **10** were observed at: H-5 (d, $J = 7.9$ Hz) 6.90–7.05 ppm; and H-6 (d, $J = 7.9$ Hz) 7.95–8.10 ppm. The carboxamide group signals of compounds **10a–d** appeared as a singlet at 11.90–12.15 ppm, whereas the signals of the sulfonamide groups appeared as a singlet at 7.30–7.35 ppm.

It should be mentioned that N-[4-(aminosulfonyl)phenyl]-1-(4-chlorophenyl)-4-oxo-1,4-dihydropyridazine-3-carboxamide **10d** was obtained earlier by another method [38]. The proton signal data in the ^1H NMR spectra of obtained compound **10d** did not match the data described in [38], while all ^1H NMR spectral data of the acids **8a–d** and amides **10a–d** correlated with ^1H NMR spectral data of the similar compounds described in [35–37,39,40]. Due to this, probably, the structure of **10d** presented in [38] is not correct. The number of signals in the ^{13}C NMR spectra of compounds **10a–d** corresponds to the number of carbon atoms in their structures, whereas the signals of carbon atoms of 4-fluorophenyl substituent in **10b** appeared as doublets. Molecular ion peaks $[\text{M}+\text{H}]^+$ and $[\text{M}-\text{H}]^-$ are usually detected in LC/MS spectra of the compounds **10a–d**.

N-[4-(Aminosulfonyl)phenyl]-6,7-dimethoxy-1-methyl-1,4-dihydroindeno[1,2-c]pyrazole-3-carboxamide **15** was obtained according to the pathway shown in Scheme 3. Compound **12** prepared by condensation reaction of 5,6-dimethoxyindan-2-one with dimethyloxalate in the presence of sodium methylate was used without additional purification to obtain 6,7-dimethoxy-1-methyl-1,4-dihydroindeno[1,2-c]pyrazole-3-carboxylate **13**, hydrolysis of which led to acid **14**. It should be also noted that some similar derivatives of 1-methyl-1,4-dihydroindeno[1,2-c]pyrazoles were described earlier [41]. Then, 6,7-dimethoxy-1-methyl-1,4-dihydroindeno[1,2-c]pyrazole-3-carboxylic acid **14** was converted into acid chloride, which, without further purification, was transformed to **15**.



Scheme 3. Synthesis of 6,7-dimethoxy-1-methyl-1,4-dihydroindeno[1,2-c]pyrazole derivatives.

The structure and composition of compounds **13–15** were confirmed by ^1H , ^{13}C NMR spectroscopy and elemental analysis. The signals of all present protons were observed in the ^1H NMR spectra of N-[4-(aminosulfonyl)phenyl]-6,7-dimethoxy-1-methyl-1,4-dihydroindeno[1,2-c]pyrazole-3-carboxamide **15**. The NH proton signal was found as singlet at 10.36 ppm, and the NCH₃ group signal and signals of two methoxy groups as a singlets at 4.18, 3.85, 3.79 ppm. The signal of the methyl group appeared as a singlet at 3.62 ppm, while aromatic proton signals were observed as singlet (7.34 ppm) and doublets (8.02, $J = 8.5$ Hz and 7.76, $J = 8.5$ Hz). The number of signals in the ^{13}C NMR spectra of compounds **13–15** corresponded to the number of carbon atoms in their structures. Molecular ion peaks $[\text{M}+\text{H}]^+$ and $[\text{M}-\text{H}]^-$ are usually detected in LC/MS spectra of compound **15**.

2.2. Biological Evaluation

All synthesized compounds were evaluated for their inhibitory activity against four human CA isoforms, which are: hCA I, hCA II, hCA IX and hCA XII (Table 1).

Table 1. Inhibition data of human CA isoforms I, II, IX and XII with compounds **4a–f**, **5a, b, d–f**, **10a–d**, **15** and **AAZ** by a stopped flow CO₂ hydrase assay.

Com/ds	R ¹	R ²	R ³	n	K _i (nM) ¹			
					hCAI	hCAII	hCAIX	hCAXII
4a	H	H	H	0	3822	866.7	450.2	271.1
4b	H	H	Me	0	93.3	308.6	78.9	372.5
4c	Me	H	H	0	221.1	16.1	8.5	250.0
4f	Cl	H	H	0	154.7	37.2	34.2	90.8
5a	H	H	H	2	88.1	31.5	93.8	188.5
5b	H	H	Me	2	344.6	16.2	16.1	329.5
5d	Me	Me	H	2	218.5	25.2	63.5	61.3
5e	Me	H	Me	2	71.4	16.2	52.3	191.2
5f	Cl	H	H	2	2150	9.1	79.4	77.3
10a	Me	H	-	-	197.9	7.4	41.6	90.8
10b	H	F	-	-	481.0	72.5	130.8	94.8
10c	Cl	H	-	-	839.7	76.3	568.8	432.8
10d	H	Cl	-	-	6.2	8.0	165.2	65.7
15	OMe	OMe	-	-	725.6	3.3	6.1	80.5
AAZ					250.0	12.1	25.8	5.7

4a–d, f; 5a, b, d–f

10a–d

15

¹ Mean from 3 different assays, by a stopped flow technique (errors were in the range of 5–10% of the reported values).

The inhibition of hCA I spanning among nanomolar to micromolar ranges, in particular, eight compounds **4b**, **4c**, **4d**, **4f**, **5d**, **5e**, **10a** and **10c** (Table 1), exhibited higher activity than reference drug acetazolamide (K_i 250 nM). The best activity among them was

achieved for compound **10d** with K_i 6.2 nM, followed by compound **5e** (K_i 71.4nM). The lowest activity was shown by compound **4a** with K_i at 3822 nM. The order of activity of these compounds against hCA I can be presented as follows: **10d** > **5e** > **5a** > **4b** > **4f** > **10a** > **5d** > **4c** > **5b** > **10b** > **15** > **10c** > **4d** > **5f** > **4a**.

According to structure–activity relationships, the presence of [(4-sulfamoylphenyl)amino]carbonyl substitute at position 3 of 1-(4-chlorophenyl)pyridazin-4(1H)-one (**10d**) is beneficial for hCA I inhibitory activity. The order of activity of phenyl-substituted pyridazine-4(1H)-one derivatives can be presented as **10d** > **10a** > **10b** > **10c**. Thus, replacement of 4-chlorobenzene by 3-tolyl resulted in compound **10a** with much lower activity than **10d**, followed by 4-fluoro- (**10b**) and 3-chlorobenzene derivatives (**10c**). The replacement of pyridazine derivative **10d** by 3-(2-hydroxy-3,5-dimethylphenyl)-N-(4-sulfamoylphenethyl)-1H-pyrazole-5-carboxamide (**5e**) decreased some activity. Removing both methyl groups from **5e** led to less-active compound (**5a**) compared with the previous one. Introduction of 2-hydroxy-4-methylbenzene to position 3 of pyrazole moiety as well as [(4-sulfamoylphenyl)amino]carbonyl substitute at position 5 (**4b**) further decreased the activity against hCA I, but this was still among the active compounds. The presence of 2-hydroxyphenyl substituent at position 3 of pyrazole ring and [N-(4-aminosulfonyl)phenyl]-5-carboxamide (**4a**) appeared to be detrimental. It is interesting to notice that for [4-(aminosulfonyl)phenyl]ethyl-1H-pyrazole carboxamides (compounds **5a–5f**), the presence of 2-OH and 3,5 dimethyl substitution of phenyl ring, respectively, is very important for hCA I inhibitory activity, while for [4-(aminosulfonyl)phenyl]-1H-pyrazole-5-carboxamides (**4a–4f**) a positive role is played by the presence of 2-OH, 4-Me substitution of phenyl ring. The K_i values against cytosolic hCA II isoform were in the range of 3.3 to 866.7 nM, and the order of activity was **15** > **10a** > **10d** > **5f** > **4d** > **5b** = **5e** > **5d** > **5a** > **4f** > **10b** > **10c** > **4c** > **4b** > **4a**. Compound **15** displayed the highest activity among others against hCA II, with K_i at 3.3 nM compared to AAZ (K_i at 12.1 nM). Furthermore, this compound was the most selective one, with a selectivity index (SI) of 219.9 towards hCA I, 2.0 compared to hCA IX and 24.4 towards hCA XII isoforms. Four compounds displayed higher activity against cytosolic hCA II isoform than reference drug AAZ.

The structure–activity relationship studies revealed that the presence of 5,6-dimethoxy-2,3-dihydro-1H-indene fused to pyrazole ring (**15**) was favorable for inhibitory activity towards hCA II isoform. Replacement of 6,7-dimethoxy-1-methyl-N-(4-sulfamoylphenyl)-1,4-dihydroindeno[1,2-c]pyrazole-3-carboxamide by 4-oxo-N-(4-sulfamoylphenyl)-1-(m-tolyl)-1,4-dihydropyridazine-3-carboxamide yielded the somewhat less active compound **10a**. Replacement of m-tolyl group by 4-chlorophenyl (**10d**) decreased the activity further. The 3-(5-chloro-2-hydroxyphenyl)-N-(4-sulfamoylphenethyl)-1H-pyrazole-5-carboxamide appeared to be less active (**5f**) compared to compound **10d**. Finally, among all compounds tested, the group (**5a–f**) appeared to be the more active compared to **4a–f** and **10a–d**. Thus, for compounds **5a–f**, the most favorable was the presence of 5-chloro-2-hydroxyphenyl substitution at position 3 of pyrazole moiety of N-{2-[4-(aminosulfonyl)phenyl]ethyl}-3-(5-chloro-2-hydroxyphenyl)-1H-pyrazole-5-carboxamide (**5f**), while the presence of 2-hydroxy substituent (**5a**) had the most negative influence on hCA II inhibitory activity. On the contrary, this compound was among the active compounds (third position in order of activity) against hCA I isoform. As far as [(4-aminosulfonyl) phenyl] 3-substituted phenyl-1H-pyrazole-5-carboxamide derivatives are concerned, the most beneficial was the 2-hydroxy-4,5-dimethylphenyl substitution at position 3 of the pyrazole moiety. Replacement of 2-hydroxy-4,5-dimethylphenyl group by 2-hydroxy-5-chlorophenyl led to less active compound **5b**, which was equipotent with compound **5e** bearing 2-hydroxy-3,5-dimethoxyphenyl substituent. Removal of both methyl groups was detrimental to the hCA II inhibitory activity, leading to the less active compound (**4a**) in this group. Finally, as regards the N-[4-(aminosulfonyl)phenyl]-1-aryl-4-oxo-1,4-dihydropyridazine-3-carboxamides (**10a–10d**), the most favorable for inhibitory activity towards hCA II appeared to be 3-methylphenyl substituent, while 3-chlorophenyl had a negative effect on activity. As regards the activity towards hCA IX isoform, the activity order of the compounds could

be presented as follows: **15** > **4c** > **5b** > **4f** > **10a** > **5e** > **5d** > **4b** > **5f** > **5a** > **10b** > **4d** > **10d** > **4a** > **10c**. The K_i values were in range of 6.1 to 568.8 nM. The best activity was again observed for compound **15**, as in case of the hCA II isoform, with K_i at 6.1 nM, followed by compound **4c** (K_i 8.5 nM). Three compounds (**4c**, **5b** and **15**) showed activity towards the hCA IX isoform better than AAZ (K_i at 25.8 nM). The lowest activity was shown by compound **10c** with K_i at 568.8 nM. According to the structure–activity relationships, the presence of 5,6-dimethoxy-2,3-dihydro-1H-indene fused to pyrazole ring (**15**), as in the case of hCA II, was beneficial for hCA IX inhibitory activity. Among three groups of compounds, it seems that 3-(2-hydroxyaryl)-1H-pyrazole-5-carboxamide **4a–d,f** and **5a,b,d–f** were more potent. Thus, for group of **4a–d,f** the presence of 2-hydroxy-5-methylphenyl substituent at position 3 of pyrazole moiety and N-[4-(aminosulfonyl) phenyl] carboxamide at the 5th position (**4c**) were positive for hCA IX inhibitory activity. Replacement of this substituent by 5-chloro-2-hydroxyphenyl (**4f**) decreased activity slightly, being in position 4 of the activity order, while removal of 5-Cl substituent was detrimental. In the group of N-[2-[4-(aminosulfonyl)phenyl]ethyl substituted phenyl-1H-pyrazole carboxamides, the most favorable substitution appeared to be 5-chloro-2-hydroxyphenyl (**5f**), followed by 2-hydroxy-3,5-dimethylphenyl (**5e**) with slightly lower activity. 2-Hydroxyphenyl substitution, as in the case of the previous group of compounds, had negative effect on hCA IX inhibitory activity. Unfortunately, these compounds showed moderate to weak inhibitory activity, with K_i in the range of 61.3–432.8 nM compared to the 25.7 nM of acetazolamide towards the hCA XII isoform. The summary of SAR is presented in Figure 3.

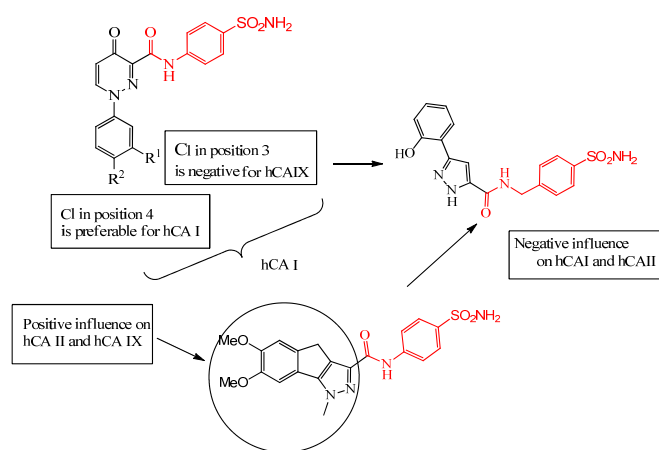


Figure 3. Structure–activity relationship summary of tested compounds.

2.3. Molecular Docking Studies

In order to predict the possible mechanism of inhibition of the tested compounds, molecular docking studies were performed on the most active compounds **5d**, **5e**, **10d** and **15** as representative of the whole set of compounds. Human CAs isoforms have analogous active sites containing His94, His96 and His119 as conserved residues, which act as zinc ligands, and conserved residues Thr199 and Glu105, which act as “gate keepers” [42–45]. Nevertheless, these isoforms differ in the residues mostly in the middle and to the exit of the active site cavity. Table 2 presents the results of the molecular docking studies of the tested compounds on hCA I, II, IX and XII isoforms. According to the docking results, all tested compounds bind the enzymes, chelating the Zn (II) ion, in a deprotonated form, as anions (negative nitrogen of the sulfonamide group) [46].

Table 2. Molecular docking free binding energies (kcal/mol) and interactions of tested compounds on hCA I, II, IX and XII isoforms.

No	R ¹	R ²	R ³	n	hCA Isoform	Estimated Free Binding Energy (Kcal/mol)	Chelating the Zn (II) Ion	Residues Involved in H-Bond Interactions	Residues Involved in Hydrophobic Interactions
5d	Me	Me	H	2	hCA I	−6.82	Yes	Thr199	Ile191, Val121, Leu198
					hCA II	−8.17	Yes	Thr199	Val121, Leu198, Thr200
					hCA IX	−6.84	Yes	Thr200	Val121, Trp209
					hCA XII	−8.10	Yes	Gln92, Ser135, Thr200	Trp5, Val121, Leu198
5e	Me	H	Me	2	hCA I	−7.16	Yes	Thr199	Ala132, Ala135, Leu198
					hCA II	−8.82	Yes	His94, Thr199	Val121, Phe131, Thr200
					hCA IX	−7.71	Yes	Thr199	Val121, Leu198, Thr200
					hCA XII	−6.21	Yes	-	Val121, Leu198
10d	H	Cl	-	-	hCA I	−12.38	Yes	Thr199	Leu198, His200, Tyr204
					hCA II	−9.11	Yes	Gln92, Thr199	Val121, Phe131, Leu198
					hCA IX	−6.55	Yes	Thr199	Val121, Leu198
					hCA XII	−7.02	Yes	His94	Val121, Ala131, Leu198
15	OMe	OMe	-	-	hCA I	−4.21	Yes	-	-
					hCA II	−9.25	Yes	Gln92, Thr200	Val121, Phe131, Leu198
					hCA IX	−10.20	Yes	Thr199, Thr200	Val121, Val131, Leu198, Thr200
					hCA XII	−7.11	Yes	Thr200	Val121, Leu198
AAZ					hCA I	−8.28	Yes	Gln92	Leu198, Thr199, His200, Pro201, Trp209
					hCA II	−8.87	Yes	Thr199, Thr200	Val121, Phe131, Leu198, Trp209
					hCA IX	−9.02	Yes	Thr199, Thr200	Val121, Val143, Val131, Leu198, Trp209
					hCA XII	−9.14	Yes	Thr199, Thr200	Val121, Val143, Leu198, Trp209

Docking studies revealed that the selectivity profile as well as the inhibition mode of some compounds to each isoform depend on the variances in the active sites of the enzymes. More precisely, the nature of the amino acids of the active site of the enzymes affects the inhibition profile of the compounds because they play an important role in the final conformation adopted and interactions formed by compounds within the enzyme active site. For example, compound **15**, with K_i value for hCA I enzyme of 725.6 nM and K_i value for hCA II of 3.3 nM, adopts a different conformation when binding both hCAs. This is probably due to the presence of the hydrophobic residue Phe131 in hCA II enzyme in contrast to the minor residue Leu131 in hCA I. Despite the fact that this smaller residue in the hCA I enzyme allows ligands to freely enter the active site of the enzyme in compound **15** with a bulky part, it is not favorable. On the other hand, residue Phe131 interacts hydrophobically with compound **15**, increasing the enzyme–ligand interactions and consequently the inhibition and selectivity of the compound to this isoform (Figure 4A). Furthermore, compound **15** forms a hydrogen bond between the sulfonamide and the backbone of Thr200 to both isoforms and another H-bond between N-atom and residue Gln92 to isoform hCA II, which further stabilizes the complex and explains the high inhibition potency (Figure 4B,C).

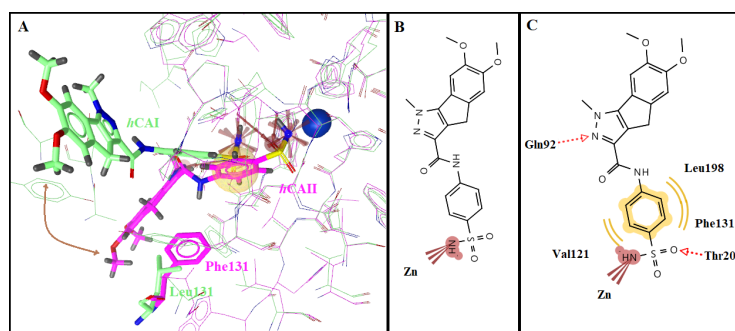


Figure 4. (A) Superposition of compound **15** bound to hCA I (green) in comparison to hCA II (magenta), with specific residues labeled. (B) 2D interaction diagram of compound **15** docking pose interactions with the key amino acids in hCA I, (C) in hCA II. Active site zinc shown as blue sphere; red dotted arrows indicate H-bond, and yellow spheres hydrophobic interactions. Orange double-headed arrow indicates the direction of conformational change of the compound bound to hCA I in comparison to hCA II enzyme.

On the other hand, compound **5d** differs from compound **15** by the presence of an ethyl -longer chain. This longer chain provides flexibility to the compound, and enables it to avoid the steric hindrance of the bulky residue Phe131 hCA II isoform, increasing the inhibition potency. This is illustrated in Figure 5 where compound **5d** in both hCA II and hCA XII isoforms adopts a conformation that favors the interactions with both active sites of the isoforms, increasing the stability of the complex and the inhibition potency (Figure 5C,D). In both structures, the negative nitrogen of the sulphonamide group chelates the Zn (II) ion and forms hydrogen bonds. In isoform hCA I, the one oxygen atom of the sulphonamide group forms a hydrogen bond with residue Thr199, while in isoform hCA XII, it forms two hydrogen bonds with residues Thr200 and Thr199. Moreover, in isoform hCA XII, the N atom of heterocycle ring forms another H-bond with residue Ser135. Additionally, the benzene moiety interacts hydrophobically with residues Val121 and Leu198 (Figure 5A,B).

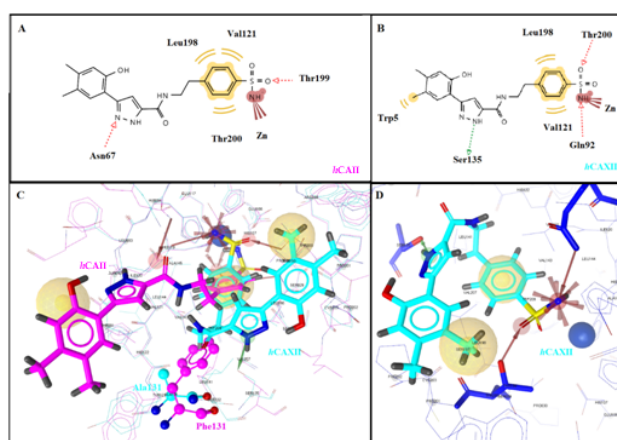


Figure 5. (A) 2D interaction diagram of compound **5d** docking pose interactions with the key amino acids in hCA II, (B) in hCA XII. (C) Superposition of compound **5d** bound to hCA II (magenta) in comparison to hCA XII (blue), with specific residues labeled. (D) 3D diagram of compound **5d** bound to hCA XII. Active site zinc shown as blue sphere, red dotted and green arrows indicate H-bond and yellow spheres hydrophobic interactions.

The docking pose of compound **10d** into the active site of hCA I isoform revealed the probable reason for its high inhibition profile. As illustrated in Figure 6, compound **10d** binds hCA I in the same manner as **AAZ**, with the negative nitrogen of the sulphonamide group chelating the Zn (II) ion. However, the benzene moiety of the compound additionally interacts hydrophobically with residues His200 and Tyr204, increasing the stability of the enzyme–compound complex, probably explaining its lower K_i value in accordance with that of reference drug **AAZ**.

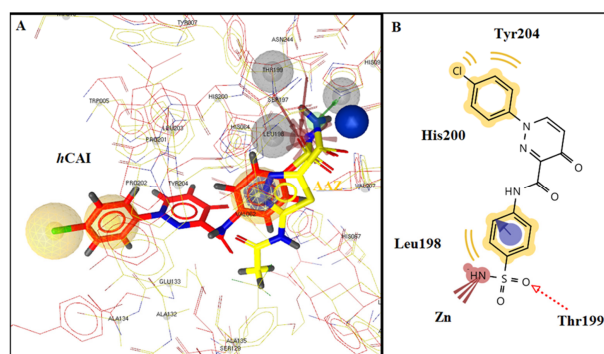


Figure 6. (A) Superposition of compound **10d** bound to hCA I (orange) in comparison to **AAZ** (yellow) in hCA I. (B) 2D interaction diagram of compound **10d** docking pose interactions with the key amino acids in hCA I. Active site zinc shown as blue sphere, red dotted arrows indicate H-bond, and yellow spheres indicate hydrophobic interactions.

3. Materials and Methods

All used solvents were of analytical grade. The ^1H and ^{13}C spectra were recorded at 298 K on a Bruker AVANCE DRX-500 spectrometer (Rheinstetten, Germany) (at 500 and 125 MHz) in solutions of (TMS as internal reference): $\text{DMSO-}d_6$, CF_3COOD and $\text{DMSO-}d_6 + 5\%(\text{mass})\text{CF}_3\text{SO}_3\text{H}$. Chemical shifts (δ) are reported in ppm, and coupling constants (J) in Hz. Chemical ionization at atmospheric pressure mass spectra (APCI) were measured with an Agilent 1200 LC/MSD SL system (Waldbronn, Germany) equipped with DAD/ELSD/LSMS-6120 diode matrix and mass-selective detector, scan range m/z 80–1000. Melting points were determined in a Fischer-Johns melting point apparatus (Pittsburgh, USA) and are uncorrected. Elemental analysis was carried out in the Analytical Laboratory of the Institute of Bioorganic and Petrochemistry of the National Academy of Sciences of Ukraine by manual methods: the carbon and hydrogen contents were determined using the Pregl gravimetric method, nitrogen was determined using the Duma's gasometrical micromethod, and sulfur was determined by the Scheininger titrimetric method.

3.1. General Procedure for the Synthesis of 3-(2-Hydroxyaryl)-1H-pyrazole-5-carboxamide 4a–d, f and 5a, b, d–f

To a solution of 2.5 mmol of the corresponding 4-oxo-4H-chromene-2-carboxylic acid 1 in 15 mL of acetonitrile, 2.5 mmol of CDI was added, and the mixture was heated at 50 °C until completion of carbon dioxide evolution. After cooling to ambient temperature, 0.374 g (2.2 mmol) of 4-aminobenzenesulfonamide or 0.44 g (2.2 mmol) 4-(2-aminoethyl)benzenesulfonamide was added to reaction mixture, which was then heated in a sealed vial for 10 h at 100 °C. After cooling to ambient temperature, the mixture was evaporated to dryness under reduced pressure. The residue was treated with 15 ml of 5% water sodium bicarbonate solution and stirred for 2 h on an ultrasonic stirrer at cooling (0–5 °C). The formed precipitate was filtered off, washed with water (10 mL) and then with ethanol (5 mL), and suspended in 15 mL of ethanol. Then, 0.63 g (6 mmol) of hydrazine hydrate was added to this suspension while stirring and the mixture was allowed to reflux for 3 h. After the cooling to ambient temperature, the resulted solution was left for 12 h, then the formed precipitate was filtered off, washed with water (10 mL), then ethanol (5 mL) and finally crystallized with DMF-ethanol mixture to yield 4a–d, f and 5a, b, d–f as colorless solids.

N-[4-(Aminosulfonyl)phenyl]-3-(2-hydroxyphenyl)-1H-pyrazole-5-carboxamide (4a). Yield 62%; m.p. 325–327 °C. $^1\text{H-NMR}$ (500 MHz, $\text{DMSO-}d_6 + 5\%(\text{mass})\text{CF}_3\text{SO}_3\text{H}$) δ : 10.33 (s, 1H, NH), 7.97 (d, $J = 8.5$ Hz, 2H, Ar), 7.79 (d, $J = 8.5$ Hz, 2H, Ar), 7.68 (d, $J = 7.7$ Hz, 1H, Ar), 7.33 (s, 1H, Ar), 7.22–7.16 (m, 1H, Ar), 6.98 (d, $J = 8.0$ Hz, 1H, Ar), 6.92–6.86 (m, 1H, Ar). $^{13}\text{C-NMR}$ (125 MHz, $\text{DMSO-}d_6 + 5\%(\text{mass})\text{CF}_3\text{SO}_3\text{H}$) δ : 160.41, 154.78, 144.61, 143.78, 142.14, 138.96, 130.08, 127.93, 126.94, 120.27, 119.85, 116.82, 116.28, 105.62. MS (APCI): $m/z = 359.0$ [M+H] $^+$; $m/z = 357.0$ [M–H]. Anal.: Calcd. for $\text{C}_{16}\text{H}_{14}\text{N}_4\text{O}_4\text{S}$ (%): C, 53.62; H, 3.94; N, 15.63; S, 8.95. Found: C, 53.51; H, 4.02; N, 15.70; S, 9.10.

N-[4-(Aminosulfonyl)phenyl]-3-(2-hydroxy-4-methylphenyl)-1H-pyrazole-5-carboxamide (4b). Yield 54%; m.p. 326–328 °C. $^1\text{H-NMR}$ (500 MHz, $\text{DMSO-}d_6 + 5\%(\text{mass})\text{CF}_3\text{SO}_3\text{H}$) δ : 10.40 (s, 1H, NH), 7.98 (d, $J = 8.5$ Hz, 2H, Ar), 7.79 (d, $J = 8.5$ Hz, 2H, Ar), 7.56 (d, $J = 7.9$ Hz, 1H, Ar), 7.29 (s, 1H, Ar), 6.71 (d, $J = 7.9$ Hz, 1H, Ar), 2.22 (s, 3H, CH_3). $^{13}\text{C-NMR}$ (125 MHz, $\text{DMSO-}d_6 + 5\%(\text{mass})\text{CF}_3\text{SO}_3\text{H}$) δ : 159.97, 154.25, 144.18, 143.41, 141.70, 139.48, 138.52, 127.29, 126.50, 120.30, 119.80, 116.77, 113.06, 104.75, 20.79. MS (APCI): $m/z = 373.2$ [M+H] $^+$; $m/z = 371.0$ [M–H]. Anal.: Calcd. for $\text{C}_{17}\text{H}_{16}\text{N}_4\text{O}_4\text{S}$ (%): C, 54.83; H, 4.33; N, 15.04; S, 8.61. Found: C, 54.90; H, 4.28; N, 14.87; S, 8.79.

N-[4-(Aminosulfonyl)phenyl]-3-(2-hydroxy-5-methylphenyl)-1H-pyrazole-5-carboxamide (4c). Yield 71%; m.p. 297–299 °C. $^1\text{H-NMR}$ (500 MHz, $\text{DMSO-}d_6 + 5\%(\text{mass})\text{CF}_3\text{SO}_3\text{H}$) δ : 10.41 (s, 1H, NH), 7.98 (d, $J = 8.7$ Hz, 2H, Ar), 7.78 (d, $J = 8.7$ Hz, 2H, Ar), 7.51 (d, $J = 2.2$ Hz, 1H, Ar), 7.32 (s, 1H, Ar), 7.00 (dd, $J = 8.2$ Hz, $J = 2.2$ Hz, 1H, Ar), 6.87 (d, $J = 8.2$ Hz, 1H, Ar), 2.23 (s, 3H, CH_3). $^{13}\text{C-NMR}$ (125 MHz, $\text{DMSO-}d_6 + 5\%(\text{mass})\text{CF}_3\text{SO}_3\text{H}$) δ : 160.49, 152.57, 144.72, 143.76, 142.18, 138.95, 130.54, 128.36, 128.04, 126.93, 120.22, 116.71, 115.90, 105.59, 20.45. MS

(APCI): $m/z = 373.0$ $[M+H]^+$; $m/z = 371.0$ $[M-H]^-$ Anal.: Calcd. for $C_{17}H_{16}N_4O_4S$ (%): C, 54.83; H, 4.33; N, 15.04; S, 8.61. Found: C, 54.95; H, 4.40; N, 14.91; S, 8.82.

N-[4-(Aminosulfonyl)phenyl]-3-(2-hydroxy-4,5-dimethylphenyl)-1H-pyrazole-5-carboxamide (**4d**). Yield 67%; m.p. 272–274 °C. 1H -NMR (500 MHz, DMSO- d_6 + 5%(mass)CF₃SO₃H) δ : 10.33 (s, 1H, NH), 7.96 (d, $J = 8.7$ Hz, 2H, Ar), 7.77 (d, $J = 8.7$ Hz, 2H, Ar), 7.44 (s, 1H, Ar), 7.27 (s, 1H, Ar), 6.75 (s, 1H, Ar), 2.16–2.12 (m, 6H, 2CH₃). ^{13}C -NMR (125 MHz, DMSO- d_6 + 5%(mass)CF₃SO₃H) δ : 160.40, 152.67, 144.62, 143.85, 142.14, 138.94, 138.42, 128.43, 127.32, 126.92, 120.21, 117.19, 113.33, 105.15, 19.73, 18.76. MS (APCI): $m/z = 387.0$ $[M+H]^+$; $m/z = 385.0$ $[M-H]^-$ Anal.: Calcd. for $C_{18}H_{18}N_4O_4S$ (%): C, 55.95; H, 4.70; N, 14.50; S, 8.30. Found: C, 55.79; H, 4.73; N, 14.35; S, 8.47.

N-[4-(Aminosulfonyl)phenyl]-3-(5-chloro-2-hydroxyphenyl)-1H-pyrazole-5-carboxamide (**4f**). Yield 75%; m.p. 302–304 °C. 1H -NMR (500 MHz, DMSO- d_6 + 5%(mass)CF₃SO₃H) δ : 10.45 (s, 1H, NH), 7.98 (d, $J = 8.8$ Hz, 2H, Ar), 7.82–7.75 (m, 3H, Ar), 7.42 (s, 1H, Ar), 7.22 (dd, $J = 8.7$ Hz, $J = 2.7$ Hz, 1H, Ar), 6.99 (d, $J = 8.7$ Hz, 1H, Ar). ^{13}C -NMR (125 MHz, DMSO- d_6 + 5%(mass)CF₃SO₃H) δ : 160.26, 153.67, 144.46, 142.56, 142.15, 139.00, 129.37, 126.97, 126.93, 123.40, 120.26, 118.51, 118.35, 106.49. MS (APCI): $m/z = 395.0$ ($[M(^{37}Cl)+H]^+$, 30); $m/z = 392.9$ ($[M(^{35}Cl)+H]^+$, 100); $m/z = 393.0$ ($[M(^{37}Cl)-H]^-$, 30); $m/z = 390.9$ ($[M(^{35}Cl)-H]^-$, 100). Anal.: Calcd. for $C_{16}H_{13}ClN_4O_4S$ (%): C, 48.92; H, 3.34; N, 14.26; S, 8.16. Found: C, 48.81; H, 3.38; N, 14.11; S, 8.33.

N-[2-[4-(Aminosulfonyl)phenyl]ethyl]-3-(2-hydroxyphenyl)-1H-pyrazole-5-carboxamide (**5a**). Yield 70%; m.p. 252–253 °C. 1H -NMR (500 MHz, DMSO- d_6) δ : 13.78 (s, 0.351H, OH), 13.17 (s, 0.65H, OH), 10.39 (s, 0.35H, NH), 10.20 (s, 0.65H, NH), 8.69 (s, 0.35H, NH), 8.13 (s, 0.65H, NH), 7.76 (d, $J = 7.9$ Hz, 2H, Ar), 7.71–7.59 (m, 1H, Ar), 7.44 (d, $J = 7.9$ Hz, 2H, Ar), 7.28 (s, 2H, NH₂), 7.24–7.16 (m, 1H, Ar), 7.11–6.90 (m, 2H, Ar), 6.94–6.86 (m, 1H, Ar), 3.59–3.49 (m, 2H, NCH₂), 2.98–2.89 (m, 2H, CH₂Ar). 1H -NMR (500 MHz, CF₃COOD) δ : 7.94–7.88 (m, 2H, Ar), 7.80–7.74 (m, 1H, Ar), 7.58 (s, 1H, Ar), 7.55–7.45 (m, 3H, Ar), 7.18–7.10 (m, 2H, Ar), 3.90 (t, $J = 7.2$ Hz, 2H, NCH₂), 3.14 (t, $J = 7.2$ Hz, 2H, CH₂Ar). 1H -NMR (500 MHz, DMSO- d_6 + 5%(mass)CF₃SO₃H) δ : 8.45 (s, 1H, NH), 7.73 (d, $J = 8.0$ Hz, 2H, Ar), 7.66–7.59 (m, 1H, Ar), 7.41 (d, $J = 8.0$ Hz, 2H, Ar), 7.24–7.11 (m, 2H, Ar), 6.96 (d, $J = 8.1$ Hz, 1H, Ar), 6.91–6.84 (m, 1H, Ar), 3.49–3.55 (m, 2H, NCH₂), 2.91 (t, $J = 7.2$ Hz, 2H, CH₂Ar). ^{13}C -NMR (125 MHz, DMSO- d_6 + 5%(mass)CF₃SO₃H) δ : 160.76, 154.98, 144.54, 144.19, 143.72, 142.43, 130.17, 129.63, 127.87, 126.19, 119.92, 116.90, 116.30, 104.61, 40.19, 35.21. MS (APCI): $m/z = 387.0$ $[M+H]^+$; $m/z = 385.0$ $[M-H]^-$. Anal.: Calcd. for $C_{18}H_{18}N_4O_4S$ (%): C, 55.95; H, 4.70; N, 14.50; S, 8.30. Found: C, 55.79; H, 4.64; N, 14.68; S, 8.54.

N-[2-[4-(Aminosulfonyl)phenyl]ethyl]-3-(2-hydroxy-4-methylphenyl)-1H-pyrazole-5-carboxamide (**5b**). Yield 64%; m.p. 254–255 °C. 1H -NMR (500 MHz, DMSO- d_6 + 5%(mass)CF₃SO₃H) δ : 8.39 (s, 1H, NH), 7.72 (d, $J = 8.0$ Hz, 2H, Ar), 7.49 (d, $J = 7.9$ Hz, 1H, Ar), 7.40 (d, $J = 8.0$ Hz, 2H, Ar), 7.14 (s, 1H, Ar), 6.76 (s, 1H, Ar), 6.71–6.68 (m, 1H, Ar), 3.52 (t, $J = 7.2$ Hz, 2H, NCH₂), 2.91 (t, $J = 7.2$ Hz, 2H, CH₂Ar), 2.22 (s, 3H, CH₃). ^{13}C -NMR (125 MHz, DMSO- d_6 + 5%(mass)CF₃SO₃H) δ : 160.62, 154.88, 144.49, 144.14, 143.67, 142.41, 140.10, 129.59, 127.68, 126.15, 120.79, 117.24, 113.39, 104.26, 40.16, 35.16, 21.28. MS (APCI): $m/z = 401.0$ $[M+H]^+$; $m/z = 399.0$ $[M-H]^-$. Anal.: Calcd. for $C_{19}H_{20}N_4O_4S$ (%): C, 56.99; H, 5.03; N, 13.99; S, 8.01. Found: C, 57.14; H, 5.08; N, 13.84; S, 8.19.

N-[2-[4-(Aminosulfonyl)phenyl]ethyl]-3-(2-hydroxy-4,5-dimethylphenyl)-1H-pyrazole-5-carboxamide (**5d**). Yield 61%; m.p. 256–258 °C. 1H -NMR (500 MHz, DMSO- d_6 + 5%(mass)CF₃SO₃H) δ : 8.46 (s, 1H, NH), 7.74 (d, $J = 8.0$ Hz, 2H, Ar), 7.45–7.33 (m, 3H, Ar), 7.17 (s, 1H, Ar), 6.75 (s, 1H, Ar), 3.55–3.49 (m, 2H, NCH₂), 2.92 (t, $J = 7.1$ Hz, 2H, CH₂Ar), 2.14–2.11 (m, 6H, 2CH₃). ^{13}C -NMR (125 MHz, DMSO- d_6 + 5%(mass)CF₃SO₃H) δ : 160.72, 152.84, 144.52, 144.12, 143.73, 142.40, 138.48, 129.56, 128.33, 127.31, 126.13, 117.87, 113.32, 104.14, 40.12, 35.16, 19.76, 18.80. MS (APCI): $m/z = 415.0$ $[M+H]^+$; $m/z = 413.1$ $[M-H]^-$. Anal.: Calcd. for $C_{20}H_{22}N_4O_4S$ (%): C, 57.96; H, 5.35; N, 13.52; S, 7.74. Found: C, 58.04; H, 5.40; N, 13.41; S, 7.92.

N-[2-[4-(Aminosulfonyl)phenyl]ethyl]-3-(2-hydroxy-3,5-dimethylphenyl)-1H-pyrazole-5-carboxamide (**5e**). Yield 65%; m.p. 273–275 °C. 1H -NMR (500 MHz, DMSO- d_6 + 5%(mass)CF₃SO₃H) δ : 8.56 (s, 1H, NH), 7.72 (d, $J = 8.1$ Hz, 2H, Ar), 7.41 (d, $J = 8.1$ Hz, 2H, Ar), 7.26 (s, 1H, Ar), 7.20 (s, 1H, Ar),

6.88 (s, 1H, Ar), 3.53–3.47 (m, 2H, NCH₂), 2.91 (t, *J* = 7.2 Hz, 2H, CH₂Ar), 2.19 (s, 3H, CH₃), 2.14 (s, 3H, CH₃). ¹³C-NMR (125 MHz, DMSO-*d*₆ +5%(mass)CF₃SO₃H) δ: 159.41, 151.33, 149.53, 144.05, 142.45, 140.27, 131.73, 129.59, 128.15, 126.16, 125.59, 124.93, 116.00, 102.78, 40.24, 35.07, 20.49, 16.4. MS (APCI): *m/z* = 415.2 [M+H]⁺; *m/z* = 413.0 [M–H][–]. Anal.: Calcd. for C₂₀H₂₂N₄O₄S (%): C, 57.96; H, 5.35; N, 13.52; S, 7.74. Found: C, 57.88; H, 5.40; N, 13.34; S, 7.96.

N-{2-[4-(Aminosulfonyl)phenyl]ethyl}-3-(5-chloro-2-hydroxyphenyl)-1H-pyrazole-5-carboxamide (**5f**). Yield 72%; m.p. 260–261 °C. ¹H-NMR (500 MHz, DMSO-*d*₆ +5%(mass)CF₃SO₃H) δ: 8.42 (s, 1H, NH), 7.75–7.68 (m, 3H, Ar), 7.41 (d, *J* = 8.0 Hz, 2H, Ar), 7.24 (s, 1H, Ar), 7.19 (dd, *J* = 8.7 Hz, *J* = 2.7 Hz, 1H, Ar), 6.96 (d, *J* = 8.7 Hz, 1H, Ar), 3.53–3.48 (m, 2H, NCH₂), 2.91 (t, *J* = 7.1 Hz, 2H, CH₂Ar). ¹³C-NMR (125 MHz, DMSO-*d*₆ +5%(mass)CF₃SO₃H) δ: 160.85, 153.79, 144.24, 143.70, 143.34, 142.41, 129.65, 129.35, 126.94, 126.20, 123.50, 118.59, 105.35, 40.18, 35.23. MS (APCI): *m/z* = 423.0 ([M(³⁷Cl)+H]⁺; 30); *m/z* = 421.0 ([M(³⁵Cl)+H]⁺, 100); *m/z* = 421.0 ([M(³⁷Cl)–H][–], 30); *m/z* = 419.0 ([M(³⁵Cl)–H][–], 100). Anal.: Calcd. for C₁₈H₁₇ClN₄O₄S (%): C, 51.37; H, 4.04; N, 13.31; S, 7.62. Found: C, 51.24; H, 4.08; N, 13.45; S, 7.75.

3.2. General Procedure for the Synthesis of 4-Oxo-1-aryl-1,4-dihydropyridazine-3-carboxylic acid **8a–d**

A solution of 30 mmol of the corresponding methyl 3-oxo-2-(arylhydrazono)butanoates **6** in 30 ml DMFDMA was refluxed for 2 h. The reaction mixture was cooled to ambient temperature and then chilled to 0 °C. The formed precipitate was filtered off, then washed with ethyl acetate (5 mL) to yield methyl 4-oxo-1-aryl-1,4-dihydropyridazine-3-carboxylates **7a–d** as a pale-yellow solids. Then, a solution of 2 g (50 mmol) of sodium hydroxide in 50 ml of water was added at 0 °C to the suspension of **7** in 130 ml of methanol and was stirred at ambient temperature for 3 h. Next, 52 ml of 1M water solution of hydrochloric acid was added to this suspension at 0 °C. The resulting mixture was concentrated under reduced pressure; the formed precipitate was filtered off, then washed with water and dried at 45–50 °C to yield **8a–d** as yellow solids.

1-(3-Methylphenyl)-4-oxo-1,4-dihydropyridazine-3-carboxylic acid (**8a**). Yield 72%; m.p. 217–219 °C. ¹H-NMR (500 MHz, DMSO-*d*₆) δ: 14.87 (s, 1H, COOH), 9.05 (d, *J* = 7.7 Hz, 1H, H-6), 7.62–7.53 (m, 2H, Ar), 7.51–7.44 (m, 1H, Ar), 7.35 (d, *J* = 7.2 Hz, 1H, Ar), 7.03 (d, *J* = 7.7 Hz, 1H, H-5), 2.42 (s, 3H, CH₃). Anal.: Calcd. for C₁₂H₁₀N₂O₃ (%): C, 62.61; H, 4.38; N, 12.17. Found: C, 62.49; H, 4.35; N, 12.09.

1-(4-Fluorophenyl)-4-oxo-1,4-dihydropyridazine-3-carboxylic acid (**8b**). Yield 65%; m.p. 227–229 °C. ¹H-NMR (500 MHz, DMSO-*d*₆) δ: 14.50 (s, 1H, COOH), 9.03 (d, *J* = 7.8 Hz, 1H, H-6), 7.91–7.79 (m, 2H, Ar), 7.47–7.35 (m, 2H, Ar), 7.02 (d, *J* = 7.8 Hz, 1H, H-5). Anal. Calcd. for C₁₁H₇FN₂O₃ (%): C, 56.42; H, 3.01; N, 11.96. Found: C, 56.33; H, 3.09; N, 11.80.

1-(3-Chlorophenyl)-4-oxo-1,4-dihydropyridazine-3-carboxylic acid (**8c**). Yield 67%; m.p. 224–226 °C. ¹H-NMR (500 MHz, DMSO-*d*₆) δ: 14.62 (s, 1H, COOH), 9.06 (d, *J* = 7.8 Hz, 1H, H-6), 7.92–7.87 (m, 1H, Ar), 7.78–7.73 (m, 1H, Ar), 7.62–7.51 (m, 2H, Ar), 7.03 (d, *J* = 7.8 Hz, 1H, H-5). Anal.: Calcd. for C₁₁H₇ClN₂O₃ (%): C, 52.71; H, 2.82; N, 11.18. Found: C, 52.79; H, 2.88; N, 11.27.

1-(4-Chlorophenyl)-4-oxo-1,4-dihydropyridazine-3-carboxylic acid (**8d**). Yield 75%; m.p. 225–227 °C. ¹H-NMR (500 MHz, DMSO-*d*₆) δ: 14.84 (s, 1H, COOH), 9.09 (d, *J* = 7.8 Hz, 1H, H-6), 7.83 (d, *J* = 8.9 Hz, 2H, Ar), 7.63 (d, *J* = 8.9 Hz, 2H, Ar), 7.02 (d, *J* = 7.8 Hz, 1H, H-5). Anal.: Calcd. for C₁₁H₇ClN₂O₃ (%): C, 52.71; H, 2.82; N, 11.18. Found: C, 52.83; H, 2.77; N, 11.31.

3.3. General Procedure for the Synthesis of 4-Oxo-1-aryl-1,4-dihydropyridazine-3-carbonyl chloride **9a–d**

To the suspension of 2 mmol of **8** in 20 mL of dry chloroform 2 mL of freshly distilled thionyl chloride and one drop of dry DMF was added. The mixture was heated for 1 h at 45–50 °C and then evaporated to dryness under reduced pressure. The residue was treated with 5 mL of dry toluene and the mixture was evaporated to dryness under reduced pressure again. The residues were used for the next step without any additional purification.

3.4. General Procedure for the Synthesis of *N*-[4-(aminosulfonyl)phenyl]-1-aryl-4-oxo-1,4-dihydropyridazine-3-carboxamide **10a–d**

To a solution of 0.17 g (1 mmol) of 4-aminobenzenesulfonamide and 0.11 g (1.1 mmol) of triethylamine in 5 mL of acetonitrile, a solution of 1 mmol of compounds **9a–d** in 10 mL acetonitrile was added while stirring and cooling to 0–5 °C. The mixture was stirred for 1 h at ambient temperature and evaporated to dryness under reduced pressure. Then, 15 mL of water was added, and the formed precipitate was filtered off, dried in air and crystallized from the DMF:ethanol mixture to yield **10a–d** as brown or yellowish-brown solids.

N-[4-(Aminosulfonyl)phenyl]-1-(3-methylphenyl)-4-oxo-1,4-dihydropyridazine-3-carboxamide (**10a**). Yield 90%; m.p. 295–297 °C. ¹H-NMR (500 MHz, DMSO-*d*₆) δ: 12.10 (s, 1H, NH), 8.98 (d, *J* = 7.8 Hz, 1H, H-6), 7.91–7.81 (m, 4H, Ar), 7.65–7.54 (m, 2H, Ar), 7.52–7.45 (m, 1H, Ar), 7.35–7.26 (m, 3H, NH₂, Ar), 6.92 (d, *J* = 7.8 Hz, 1H, H-5), 2.42 (s, 3H, CH₃). MS (APCI): *m/z* = 385.0 [M+H]⁺; *m/z* = 383.0 [M–H][–]. Anal.: Calcd. for C₁₈H₁₆N₄O₄S (%): C, 56.24; H, 4.20; N, 14.57; S, 8.34. Found: C, 56.19; H, 4.28; N, 14.39; S, 8.51.

N-[4-(Aminosulfonyl)phenyl]-1-(4-fluorophenyl)-4-oxo-1,4-dihydropyridazine-3-carboxamide (**10b**). Yield 90%; m.p. 313–315 °C. ¹H-NMR (500 MHz, DMSO-*d*₆) δ: 12.11 (s, 1H, NH), 8.97 (d, *J* = 7.8 Hz, 1H, H-6), 7.92–7.78 (m, 6H, Ar), 7.51–7.42 (m, 2H, Ar), 7.33 (s, 2H, NH₂), 6.93 (d, *J* = 7.8 Hz, 1H, H-5). ¹³C-NMR (126 MHz, DMSO-*d*₆) δ: 169.29, 161.64 (d, *J*_{CF} = 246.4 Hz), 159.97, 147.22, 142.10, 140.96, 139.46, 139.33, 126.97, 123.92 (d, *J*_{CF} = 9.0 Hz), 120.61, 119.52, 116.53 (d, *J*_{CF} = 23.4 Hz). MS (APCI): *m/z* = 389.0 [M+H]⁺; *m/z* = 387.0 [M–H][–]. Anal.: Calcd. for C₁₇H₁₃FN₄O₄S (%): C, 52.57; H, 3.37; N, 14.43; S, 8.26. Found: 52.69; H, 3.31; N, 14.28; S, 8.47.

N-[4-(Aminosulfonyl)phenyl]-1-(3-chlorophenyl)-4-oxo-1,4-dihydropyridazine-3-carboxamide (**10c**). Yield 82%; m.p. 297–299 °C. ¹H-NMR (500 MHz, DMSO-*d*₆) δ: 11.98 (s, 1H, NH), 9.05 (d, *J* = 7.9 Hz, 1H, H-6), 7.95 (d, *J* = 2.1 Hz, 1H, Ar), 7.91–7.78 (m, 5H, Ar), 7.69–7.56 (m, 2H, Ar), 7.32 (s, 2H, NH₂), 6.93 (d, *J* = 7.9 Hz, 1H, H-5). ¹³C-NMR (126 MHz, DMSO-*d*₆) δ: 169.82, 160.34, 147.97, 144.21, 142.16, 141.36, 139.80, 134.43, 131.81, 128.86, 127.39, 121.71, 120.90, 120.37, 119.96. MS (APCI): *m/z* = 406.9 ([M(³⁷Cl)+H]⁺; 30); *m/z* = 404.9 ([M(³⁵Cl)+H]⁺, 100); *m/z* = 405.0 ([M(³⁷Cl)–H][–], 30); *m/z* = 402.9 ([M(³⁵Cl)–H][–], 100). Anal.: Calcd. for C₁₇H₁₃ClN₄O₄S (%): C, 50.44; H, 3.24; N, 13.84; S, 7.92. Found: C, 50.29; H, 3.31; N, 13.65; S, 8.09.

N-[4-(Aminosulfonyl)phenyl]-1-(4-chlorophenyl)-4-oxo-1,4-dihydropyridazine-3-carboxamide (**10d**). Yield 90%; m.p. 310–312 °C (lit. 190 °C [7]). ¹H-NMR (500 MHz, DMSO-*d*₆) δ: 12.03 (s, 1H, NH), 9.01 (d, *J* = 7.8 Hz, 1H, H-6), 7.93–7.81 (m, 6H, Ar), 7.68 (d, *J* = 8.7 Hz, 2H, Ar), 7.32 (s, 2H, NH₂), 6.93 (d, *J* = 7.8 Hz, 1H, H-5). ¹³C-NMR (126 MHz, DMSO-*d*₆) δ: 169.27, 159.93, 147.51, 141.66, 141.59, 140.92, 139.33, 133.04, 129.63, 126.93, 123.06, 120.52, 119.48. MS (APCI): *m/z* = 407.0 ([M(³⁷Cl)+H]⁺; 30); *m/z* = 405.0 ([M(³⁵Cl)+H]⁺, 100); *m/z* = 405.0 ([M(³⁷Cl)–H][–], 30); *m/z* = 403.0 ([M(³⁵Cl)–H][–], 100). Anal.: Calcd. for C₁₇H₁₃ClN₄O₄S (%): C, 50.44; H, 3.24; N, 13.84; S, 7.92. Found: C, 50.47; H, 3.29; N, 13.68; S, 8.13.

3.5. Synthesis of *N*-[4-(aminosulfonyl)phenyl]-6,7-dimethoxy-1-methyl-1,4-dihydroindeno[1,2-*c*]pyrazole-3-carboxamide **15**

Sodium 1-(5,6-dimethoxy-1-oxo-1,3-dihydro-2H-inden-2-ylidene)-2-methoxy-2-oxoethanolate (**12**). A solution of 5.76 g (30 mmol) of 5,6-dimethoxyindan-1-one **11** and 4.72 g (40 mmol) of dimethyl oxalate in 50 mL methanol was added in one portion to a solution of 2.7 g (50 mmol) of sodium methylate in 30 mL of methanol. The reaction mixture was heated for 2 h at 55–60 °C, cooled to ambient temperature and then chilled to 0 °C. The formed precipitate was filtered off, washed with methanol (10 mL) and then diethyl ether (5 mL) to yield **12** as a yellow solid. It was used for the next step without additional purification.

Methyl 6,7-dimethoxy-1-methyl-1,4-dihydroindeno[1,2-*c*]pyrazole-3-carboxylate (**13**). To a stirred solution of 2.48 g (30 mmol) of methylhydrazine hydrochloride in 50 mL of methanol and 10 mL of glacial acetic acid, 7.5 g (25 mmol) of **12** was added. The mixture was heated for 12 h at 60 °C, evaporated to dryness under reduced pressure, and the resulting residue

was treated with 50 mL of water. The formed precipitate was filtered off, washed with water (10 mL), then methanol (5 mL) and finally twice crystallized from methanol to afford 13 as a colorless solid. Yield 55%; m.p. 187–188 °C. ¹H-NMR (500 MHz, DMSO-*d*₆) δ: 7.32 (s, 1H, Ar), 7.23 (s, 1H, Ar), 4.13 (s, 3H, CH₃), 3.85 (s, 3H, CH₃), 3.81 (s, 3H, CH₃), 3.80 (s, 3H, CH₃), 3.55 (s, 2H, CH₂). ¹³C-NMR (125 MHz, DMSO-*d*₆) δ: 162.59, 150.30, 148.66, 148.63, 141.40, 135.77, 128.59, 124.01, 110.96, 103.98, 56.52, 56.18, 51.90, 38.67, 29.47. Anal.: Calcd. for C₁₅H₁₆N₂O₄ (%): C, 62.49; H, 5.59; N, 9.72. Found (%): C, 62.55; H, 5.51; N, 9.83.

*6,7-Dimethoxy-1-methyl-1,4-dihydroindeno[1,2-*c*]pyrazole-3-carboxylic acid (14)*. A stirred solution of 2.88 g (10 mmol) of compound 13 in 30 mL of methanol was treated with a solution of 1.68 g (30 mmol) of potassium hydroxide in 15 mL water. The resulting mixture was stirred at 50 °C for 18 h (TLC control), cooled to ambient temperature and acidified with formic acid. The formed precipitate was filtered off, washed with water, dried in air and crystallized from ethanol to yield 14 as colorless solid. Yield 91%; m.p. 235–236 °C. ¹H-NMR (500 MHz, DMSO-*d*₆,) δ: 12.60 (s, 1H, COOH), 7.28 (s, 1H, Ar), 7.19 (s, 1H, Ar), 4.10 (s, 3H, CH₃), 3.83 (s, 3H, CH₃), 3.78 (s, 3H, CH₃), 3.50 (s, 2H, CH₂). ¹³C-NMR (125 MHz, DMSO-*d*₆) δ: 163.64, 150.15, 148.59, 148.49, 141.47, 136.85, 128.64, 124.16, 110.92, 103.86, 56.48, 56.14, 38.54, 29.48. MS (APCI): *m/z* = 275.1 [M+H]⁺; *m/z* = 273.1 [M-H]⁻. Calcd. for C₁₄H₁₄N₂O₄ (%): C, 61.31; H, 5.14; N, 10.21 Found (%): C, 61.43; H, 5.19; N, 10.08.

*N-[4-(Aminosulfonyl)phenyl]-6,7-dimethoxy-1-methyl-1,4-dihydroindeno[1,2-*c*]pyrazole-3-carboxamide (15)*. To a stirred solution of 0.28 g (1 mmol) of 14 in 10 mL of anhydrous toluene 1 mL of thionyl chloride was added. The mixture was heated for 1 h at 80 °C and then evaporated to dryness under reduced pressure. The residue was treated with 5 mL of toluene and the resulted mixture was continuously evaporated to dryness under reduced pressure again. The residue was dissolved in 10 mL of acetonitrile and then was added to a solution of 0.17 g (1 mmol) of 4-aminobenzenesulfonamide and 0.11 g (1.1 mmol) of triethylamine in 5 mL acetonitrile while stirring and cooling (0–5 °C). The mixture was stirred for 1 h, evaporated to dryness under reduced pressure, residue was treated with 15 mL of water, the formed precipitate was filtered off, dried at air and crystallized from the DMF:ethanol mixture (1:7 *v/v*) to yield 15 as colorless solid. Yield 90%; m.p. 286–287 °C. ¹H-NMR (500 MHz, DMSO-*d*₆) δ: 10.36 (s, 1H, NH), 8.02 (d, *J* = 8.5 Hz, 2H, Ar), 7.76 (d, *J* = 8.5 Hz, 2H, Ar), 7.34 (s, 1H, Ar), 7.28–7.21 (m, 3H, Ar, NH₂), 4.18 (s, 3H, CH₃), 3.85 (s, 3H, CH₃), 3.79 (s, 3H, CH₃), 3.62 (s, 2H, CH₂). ¹³C-NMR (125 MHz, DMSO-*d*₆) δ: 160.96, 151.00, 148.70, 148.63, 142.33, 141.88, 139.33, 138.82, 127.55, 126.85, 123.96, 120.05, 110.97, 104.06, 56.56, 56.16, 38.50, 29.43. MS (APCI): *m/z* = 429.0 [M+H]⁺; *m/z* = 427.0 [M-H]⁻. Anal.: Calcd. for C₂₀H₂₀N₄O₅S (%): C, 56.07; H, 4.70; N, 13.08; S, 7.48. Found: C, 55.92; H, 4.78; N, 12.95; S, 7.61.

3.6. Molecular Docking Studies

Molecular modeling studies were performed using the software AutoDock 4.2 [47]. Protein Data Bank was also used in order to obtain the he crystal structures of *h*CA I (PDB code 3W6H) and *h*CA II (PDB code 3HS4) cytosolic isoforms as well as *h*CA IX (PDB code 3IAI) and *h*CA XII (PDB code 1JD0) transmembrane tumor-associated isoforms [48]. All of the procedure was carried out as described in our previous work [49].

3.7. CA Inhibition Assay

An Applied Photophysics stopped-flow instrument was used for assaying the CA-catalyzed CO₂ hydration activity [50]. Phenol red (at a concentration of 0.2 mM) was used as an indicator, working at the absorbance maximum of 557 nm, with 20 mM Hepes (pH 7.4) as a buffer, and 20 mM Na₂SO₄ (for maintaining constant ionic strength), following the initial rates of the CA-catalyzed CO₂ hydration reaction for a period of 10–100 s. The CO₂ concentrations ranged from 1.7 to 17 mM for the determination of the kinetic parameters and inhibition constants [48]. The non-catalyzed CO₂ hydration was not subtracted from these curves and accounted for the remaining observed activity even at

high concentration of inhibitor, being in the range of 16–25%. However, the background activity from the uncatalyzed reaction was always subtracted when IC₅₀ values were obtained by using the data analysis software for the stopped-flow instrument. Enzyme concentrations ranged between 5 nM and 12 nM. For each inhibitor, at least six traces of the initial 5–10% of the reaction were used for determining the initial velocity. The uncatalyzed rates were determined in the same manner and subtracted from the total observed rates. Stock solutions of the inhibitor (0.1 mM) were prepared in distilled–deionized water, and dilutions up to 0.01 nM were performed thereafter with the assay buffer. Inhibitor and enzyme solutions were preincubated together for 15 min at room temperature prior to the assay, to allow for the formation of the E–I complex. The inhibition constants were obtained by nonlinear least-squares methods using PRISM 3 and the Cheng–Prusoff equation as reported earlier and represented the mean from at least three different determinations. All CA isoforms were recombinant proteins obtained in-house, as reported earlier [2,51,52].

4. Conclusions

In conclusion, we synthesized and investigated a novel series of sulfonamides incorporating pyrazole- and pyridazinecarboxamide moieties for their effective inhibition against different and most relevant human carbonic anhydrase isoforms such as the ubiquitous hCA I, hCA II, and tumor associated isoforms hCA IX and XII, which are involved in a variety of diseases such as glaucoma, retinitis pigmentosa, epilepsy, and tumors. Compound **4c** showed a good selectivity index of 26 on hCA IX compared to hCA I and two times compared to hCA II. On the other hand, compound **10f** was shown to be the most active on hCA II with an SI of 236 compared to hCA I and 8.7 compared to hCA IX. These interesting features make them good candidates for preclinical evaluation in glaucoma or various tumors in which the two enzymes (hCA II and hCA IX) are involved. Furthermore, computational procedures were used to investigate the binding mode of this class of compounds.

Supplementary Materials: The following are available online: Copies of ¹H, ¹³C NMR and LCMS Spectra of Products (Figures S1A–S19C).

Author Contributions: Conceptualization, A.G. and V.K.; methodology, C.T.S.; software, A.P.; validation, A.P.; formal analysis, R.V. and S.P.; investigation, V.B. and A.A.; data curation, V.B. and C.T.S.; writing—original draft preparation, V.B., A.A., M.P., C.T.S. and A.G.; writing—review and editing, A.A., C.T.S. and A.G.; supervision, C.T.S. and A.G. All authors have read and agreed to the published version of the manuscript.

Funding: This research received no external funding.

Institutional Review Board Statement: Not applicable.

Informed Consent Statement: Not applicable.

Data Availability Statement: Not applicable.

Conflicts of Interest: The authors declare no conflict of interest.

Sample Availability: Samples of the compounds are available from the authors.

References

1. Quade, B.N.; Parker, M.D.; Occhipinti, R. The therapeutic importance of acid-base balance. *Biochem. Pharmacol.* **2021**, *183*, 114278. [[CrossRef](#)] [[PubMed](#)]
2. Supuran, C.T. Carbonic anhydrases: Novel therapeutic applications for inhibitors and activators. *Nat. Rev. Drug Discov.* **2008**, *7*, 168–181. [[CrossRef](#)]
3. Supuran, C.T. Emerging role of carbonic anhydrase inhibitors. *Clin. Sci.* **2021**, *135*, 1233–1249. [[CrossRef](#)]
4. Xu, Y.; Feng, L.; Jeffrey, P.D.; Shi, Y.; Morel, F.M. Structure and metal exchange in the cadmium carbonic anhydrase of marine diatoms. *Nature* **2008**, *452*, 56–61. [[CrossRef](#)] [[PubMed](#)]
5. Capasso, C.; Supuran, C.T. An overview of the alpha-, beta- and gamma-carbonic anhydrases from bacteria: Can bacterial carbonic anhydrases shed new light on evolution of bacteria? *J. Enzym. Inhib. Med. Chem.* **2015**, *30*, 325–332. [[CrossRef](#)]

6. Supuran, C.T.; Capasso, C. The eta-class carbonic anhydrases as drug targets for antimalarial agents. *Expert. Opin. Ther. Targets* **2015**, *19*, 551–563. [[CrossRef](#)] [[PubMed](#)]
7. Akgul, O.; Di Cesare Mannelli, L.; Vullo, D.; Angeli, A.; Ghelardini, C.; Bartolucci, G.; Alfawaz Altamimi, A.S.; Scozzafava, A.; Supuran, C.T.; Carta, F. Discovery of novel nonsteroidal anti-inflammatory drugs and carbonic anhydrase inhibitors hybrids (NSAIDs-CAIs) for the management of rheumatoid arthritis. *J. Med. Chem.* **2018**, *61*, 4961–4977. [[CrossRef](#)]
8. Bua, S.; Di Cesare Mannelli, L.; Vullo, D.; Ghelardini, C.; Bartolucci, G.; Scozzafava, A.; Supuran, C.T.; Carta, F. Design and synthesis of novel Nonsteroidal Anti-Inflammatory Drugs and Carbonic Anhydrase Inhibitors hybrids (NSAIDs-CAIs) for the treatment of rheumatoid arthritis. *J. Med. Chem.* **2017**, *60*, 1159–1170. [[CrossRef](#)]
9. Lardner, A. The effects of extracellular pH on immune function. *J. Leukoc. Biol.* **2001**, *69*, 522–530.
10. McDonald, P.C.; Chafe, S.C.; Brown, W.S.; Saberi, S.; Swayampakula, M.; Venkateswaran, G.; Nemirovsky, O.; Gillespie, J.A.; Karasinska, J.M.; Kalloger, S.E.; et al. Regulation of pH by Carbonic Anhydrase 9 Mediates Survival of Pancreatic Cancer Cells with Activated KRAS in Response to Hypoxia. *Gastroenterology* **2019**, *157*, 823–837. [[CrossRef](#)]
11. Supuran, C.T. Carbonic anhydrase inhibitors as emerging agents for the treatment and imaging of hypoxic tumors. *Expert Opin. Investig. Drugs* **2018**, *27*, 963–970. [[CrossRef](#)] [[PubMed](#)]
12. Supuran, C.T.; Winum, J.Y. Carbonic anhydrase IX inhibitors in cancer therapy: An update. *Future Med. Chem.* **2015**, *7*, 1407–1414. [[CrossRef](#)] [[PubMed](#)]
13. Penning, T.D.; Talley, J.J.; Bertenshaw, S.R.; Carter, J.S.; Collins, P.W.; Doctor, S.; Graneto, M.J.; Lee, L.F.; Malecha, J.W.; Miyashiro, J.M.; et al. Synthesis and biological evaluation of the 1,5-diarylpyrazole class of cyclooxygenase-2 inhibitors: Identification of 4-[5-(4-methylphenyl)-3-(trifluoromethyl)-1H-pyrazol-1-yl]benzenesulfonamide (SC-58635, celecoxib). *J. Med. Chem.* **1997**, *40*, 1347–1365. [[CrossRef](#)]
14. Fioravanti, R.; Bolasco, A.; Manna, F.; Rossi, F.; Orallo, F.; Ortuso, F.; Alcaro, S.; Cirilli, R. Synthesis and biological evaluation of N-substituted-3,5-diphenyl-2-pyrazoline derivatives as cyclooxygenase (COX-2) inhibitors. *Eur. J. Med. Chem.* **2010**, *45*, 6135–6138. [[CrossRef](#)]
15. Riedel, R. Lonazolac-Ca = Calcium [3-(p-chlorophenyl)-1-phenylpyrazole-4]-acetate 1 Pharmacological properties of a new antiinflammatory/antirheumatic drug (author's transl). *Arzneim. Forsch.* **1981**, *31*, 655–665.
16. Isidro, M.L.; Cordido, F. Drug treatment of obesity: Established and emerging therapies. *Mini-Rev. Med. Chem.* **2009**, *9*, 664–673. [[CrossRef](#)] [[PubMed](#)]
17. Devi, N.; Shankar, R.; Singh, V. 4-Formyl-Pyrazole-3-Carboxylate: A Useful Aldo-X Bifunctional Precursor for the Syntheses of Pyrazole-fused/Substituted Frameworks. *J. Heterocycl. Chem.* **2018**, *55*, 373–390. [[CrossRef](#)]
18. Katz, R.J. Effects of zometapine, a structurally novel antidepressant, in an animal model of depression. *Pharmacol. Biochem. Behav.* **1984**, *21*, 487–490. [[CrossRef](#)]
19. Lippa, A.; Czobor, P.; Stark, J.; Beer, B.; Kostakis, E.; Gravielle, M.; Bandyopadhyay, S.; Russek, S.J.; Gibbs, T.T.; Farb, D.H.; et al. Selective anxiolysis produced by ocinaplon, a GABAA receptor modulator. *Proc. Natl. Acad. Sci. USA* **2005**, *102*, 7380–7385. [[CrossRef](#)]
20. Marinescu, M. Synthesis of Antimicrobial Benzimidazole-Pyrazole Compounds and Their Biological Activities. *Antibiotics* **2021**, *10*, 1002. [[CrossRef](#)]
21. Çetin, A.; Bildirici, I. A study on synthesis and antimicrobial activity of 4-acyl-pyrazoles. *J. Saudi Chem. Soc.* **2018**, *22*, 279–296. [[CrossRef](#)]
22. Muhammad, Z.A.; Alshehrei, F.; Zayed, M.E.M.; Farghaly, T.A.; Abdallah, M.A. Synthesis of Novel Bis-pyrazole Derivatives as Antimicrobial Agents. *Mini Rev. Med. Chem.* **2019**, *19*, 1276–1290. [[CrossRef](#)]
23. Da Costa, L.; Scheers, E.; Coluccia, A.; Casulli, A.; Roche, M.; Di Giorgio, C.; Neyts, J.; Terme, T.; Cirilli, R.; La Regina, G.; et al. Structure-Based Drug Design of Potent Pyrazole Derivatives against Rhinovirus Replication. *J. Med. Chem.* **2018**, *61*, 8402–8416. [[CrossRef](#)]
24. Corona, A.; Onnis, V.; Deplano, A.; Bianco, G.; Demurtas, M.; Distinto, S.; Cheng, Y.C.; Alcaro, S.; Esposito, F.; Tramontano, E. Design, synthesis and antiviral evaluation of novel heteroarylcarbothioamide derivatives as dual inhibitors of HIV-1 reverse transcriptase-associated RNase H and RDDP functions. *Pathog. Dis.* **2017**, *75*, ftx078. [[CrossRef](#)] [[PubMed](#)]
25. Naim, M.J.; Alam, O.; Alam, M.J.; Hassan, M.Q.; Siddiqui, N.; Naidu, V.G.M.; Alam, M.I. Design, synthesis and molecular docking of thiazolidinedione based benzene sulphonamide derivatives containing pyrazole core as potential anti-diabetic agents. *Bioorg. Chem.* **2018**, *76*, 98–112. [[CrossRef](#)]
26. Faidallah, H.M.; Al-Mohammadi, M.M.; Alamry, K.A.; Khan, K.A. Synthesis and biological evaluation of fluoropyrazolesulfonylurea and thiourea derivatives as possible antidiabetic agents. *J. Enzyme Inhib. Med. Chem.* **2016**, *31*, 157–163. [[CrossRef](#)]
27. Li, X.; Yu, Y.; Tu, Z. Pyrazole Scaffold Synthesis, Functionalization, and Applications in Alzheimer's Disease and Parkinson's Disease Treatment (2011–2020). *Molecules* **2021**, *26*, 1202. [[CrossRef](#)]
28. Grewal, A.S.; Sharma, S.K.; Pandita, D.; Lather, V. Synthesis, Docking and Evaluation of Novel Pyrazole Carboxamide Derivatives as Multifunctional Anti-Alzheimer's Agents. *J. Med. Chem. Toxicol.* **2017**, *2*, 47–54.
29. Meta, E.; Brullo, C.; Tonelli, M.; Franzblau, S.G.; Wang, Y.; Ma, R.; Baojie, W.; Orena, B.S.; Pasca, M.R.; Bruno, O. Pyrazole and imidazo[1,2-b]pyrazole Derivatives as New Potential Antituberculosis Agents. *Med. Chem.* **2019**, *15*, 17–27. [[CrossRef](#)] [[PubMed](#)]
30. Xu, Z.; Gao, C.; Ren, Q.C.; Song, X.F.; Feng, L.S.; Lv, Z.S. Recent advances of pyrazole-containing derivatives as anti-tubercular agents. *Eur. J. Med. Chem.* **2017**, *139*, 429–440. [[CrossRef](#)]

31. Bekhit, A.A.; Saudi, M.N.; Hassan, A.M.; Fahmy, S.M.; Ibrahim, T.M.; Ghareeb, D.; El-Seidy, A.M.; Al-Qallaf, S.M.; Habib, H.J.; Bekhit, A.E.A. Synthesis, molecular modeling and biological screening of some pyrazole derivatives as antileishmanial agents. *Future Med. Chem.* **2018**, *10*, 2325–2344. [CrossRef]
32. Cagide, F.; Oliveira, C.; Reis, J.; Borges, F. Optimizing the synthetic route of chromone-2-carboxylic acids: A step forward to speed-up the discovery of chromone-based multitarget-directed ligands. *Molecules* **2019**, *24*, 4214. [CrossRef]
33. Ruhemann, S.; Wragg, E. CXXV.—Condensation of phenols with esters of the acetylene series. Part VI. *J. Chem. Soc. Trans.* **1901**, *79*, 1185–1191. [CrossRef]
34. Golovchenko, A.V.; Solomyanni, R.N.; Brovarets, V.S. Synthesis of C-heteryl-substituted aminomethylphosphonic acids derivatives. *Russ. J. Gen. Chem.* **2010**, *80*, 723–727. [CrossRef]
35. Plescia, S.; Daidone, G.; Fabra, J.; Sprio, V. Studies on the synthesis of heterocyclic compounds. Part V. A novel synthesis of some pyridazin-4-(1H)one derivatives and their reaction with hydrazine. *J. Het. Chem.* **1981**, *18*, 333–334. [CrossRef]
36. Wang, L.X.; Liu, X.; Xu, S.; Tang, Q.; Duan, Y.; Xiao, Z.; Zhi, J.; Jiang, L.; Zheng, P.; Zhu, W. Discovery of novel pyrrolo-pyridine/pyrimidine derivatives bearing pyridazinone moiety as c-Met kinase inhibitors. *Eur. J. Med. Chem.* **2017**, *141*, 538–551. [CrossRef] [PubMed]
37. Liu, X.; Kou, J.; Xiao, Z.; Tian, F.; Hu, J.; Zheng, P.; Zhu, W. Design, synthesis and biological evaluation of 6,7-disubstituted-4-phenoxyquinoline derivatives bearing pyridazinone moiety as c-met inhibitors. *Molecules* **2018**, *23*, 1543. [CrossRef] [PubMed]
38. Altalbawy, F.M.A. Synthesis, in vitro antimicrobial and anticancer evaluation of some new pyridazines and polyfunctionally substituted heterocyclic compounds. *Asian J. Chem.* **2015**, *27*, 4361–4368. [CrossRef]
39. Kunitomo, J.; Yoshikawa, M.; Fushimi, M.; Kawada, A.; Quinn, J.F.; Oki, H.; Kokubo, H.; Kondo, M.; Nakashima, K.; Kamiguchi, N.; et al. Discovery of 1-[2-fluoro-4-(1H-pyrazol-1-yl)phenyl]-5-methoxy-3-(1-phenyl-1H-pyrazol-5-yl)pyridazin-4(1H)-one (tak-063), a highly potent, selective, and orally active phosphodiesterase 10a (pde10a) inhibitor. *J. Med. Chem.* **2014**, *57*, 9627–9643. [CrossRef]
40. Wang, L.; Xu, S.; Chen, X.; Liu, X.; Duan, Y.; Kong, D.; Zhao, D.; Zheng, P.; Tang, Q.; Zhu, W. Synthesis and bioevaluation study of novel N-methylpicolinamide and thienopyrimidine derivatives as selectivity c-Met kinase inhibitors. *Bioorg. Med. Chem.* **2018**, *26*, 245–256. [CrossRef]
41. Pinna, G.A.; Pirisi, M.A.; Mussinu, J.-M.; Murineddu, G.; Loriga, G.; Pau, A.; Grella, G.E. Chromophore-modified bis-benzo[g]indole carboxamides: Synthesis and antiproliferative activity of bis-benzo[g]indazole-3-carboxamides and related dimers. *Il Farmaco* **2003**, *58*, 749–763. [CrossRef]
42. Alterio, V.; Hilvo, M.; Di Fiore, A.; Supuran, C.T.; Pan, P.; Parkkila, S.; Scaloni, A.; Pastorek, J.; Patorekova, S.; Pedone, C.; et al. Crystal structure of the catalytic domain of the tumor associated human carbonic anhydrase IX. *Proc. Natl. Acad. Sci. USA* **2009**, *106*, 16233–16238. [CrossRef]
43. Di Fiore, A.; Truppo, E.; Supuran, C.T.; Alterio, V.; Dathan, N.; Booterabi, F.; Parkkila, S.; Monti, S.M.; De Simone, G. Crystal structure of the C183S/C217S mutant of human CA VII in complex with acetazolamide. *Bioorg. Med. Chem. Lett.* **2010**, *20*, 5023–5026. [CrossRef]
44. Whittington, D.A.; Waheed, A.; Ulmasov, B.; Shah, G.N.; Grubb, J.H.; Sly, W.S.; Christianson, D.W. Crystal structure of the dimeric extracellular domain of human carbonic anhydrase XII, a bitopic membrane protein overexpressed in certain cancer tumor cells. *Proc. Natl. Acad. Sci. USA* **2001**, *98*, 9545–9550. [CrossRef] [PubMed]
45. Supuran, C.T. Structure-based drug discovery of carbonic anhydrase inhibitors. *J. Enzyme Inhib. Med. Chem.* **2012**, *27*, 759–772. [CrossRef]
46. Kanamori, K.; Roberts, J.D. Nitrogen-15 nuclear magnetic resonance study of benzenesulfonamide and cyanate binding to carbonic anhydrase. *Biochemistry* **1983**, *22*, 2658–2664. [CrossRef] [PubMed]
47. Morris, G.M.; Huey, R.; Lindstrom, W.; Sanner, M.F.; Belew, R.K.; Goodsell, D.S.; Olson, A.J. Autodock4 and AutoDockTools4: Automated docking with selective receptor flexibility. *J. Comput. Chem.* **2009**, *16*, 2785–2791. [CrossRef] [PubMed]
48. Available online: <http://www.rcsb.org/> (accessed on 19 June 2021).
49. Angeli, A.; Kartsev, V.; Petrou, A.; Pinteala, M.; Brovarets, V.; Slyvchuk, S.; Pilyo, S.; Geronikaki, A.; Supuran, C.T. Chromene-Containing Aromatic Sulfonamides with Carbonic Anhydrase Inhibitory Properties. *Int. J. Mol. Sci.* **2021**, *22*, 5082. [CrossRef]
50. Khalifah, R.G. The carbon dioxide hydration activity of carbonic anhydrase. *J. Biol. Chem.* **1971**, *246*, 2561–2573. [CrossRef]
51. Abdel-Aziz, A.A.; Angeli, A.; El-Azab, A.S.; Abu El-Enin, M.A.; Supuran, C.T. Synthesis and biological evaluation of cyclic imides incorporating benzenesulfonamide moieties as carbonic anhydrase I, II, IV and IX inhibitors. *Bioorg. Med. Chem.* **2017**, *25*, 1666–1671. [CrossRef]
52. Gul, H.I.; Yamali, C.; Bulbuller, M.; Kirmizibayrak, P.B.; Gul, M.; Angeli, A.; Bua, S.; Supuran, C.T. Anticancer effects of new dibenzenesulfonamides by inducing apoptosis and autophagy pathways and their carbonic anhydrase inhibitory effects on hCA I, hCA II, hCA IX, hCA XII isoenzymes. *Bioorg. Chem.* **2018**, *78*, 290–297. [CrossRef] [PubMed]